• Clinical Research •

Three-dimensional choroidal vascularity index and choroidal thickness in fellow eyes of acute and chronic primary angle-closure using swept-source optical coherence tomography

Hai-Li Huang[1], *Guan-Hong Wang*[1], *Liang-Liang Niu*[1], *Xing-Huai Sun*[1,2,3]

[1]Department of Ophthalmology & Visual Science, Eye & ENT Hospital, Shanghai Medical College, Fudan University, Shanghai 200031, China

[2]State Key Laboratory of Medical Neurobiology and MOE Frontiers Center for Brain Science, Institutes of Brain Science, Fudan University, Shanghai 200032, China

[3]NHC Key Laboratory of Myopia, Chinese Academy of Medical Sciences, and Shanghai Key Laboratory of Visual Impairment and Restoration (Fudan University), Shanghai 200031, China

Co-first authors: Hai-Li Huang and Guan-Hong Wang

Correspondence to: Xing-Huai Sun. Department of Ophthalmology & Visual Science, Eye & ENT Hospital, Shanghai Medical College, Fudan University, Shanghai 200031, China. xhsun@shmu.edu.cn

Received: 2023-06-25 Accepted: 2023-11-28

Abstract

● **AIM:** To compare the three-dimensional choroidal vascularity index (CVI) and choroidal thickness between fellow eyes of acute primary angle-closure (F-APAC) and chronic primary angle-closure glaucoma (F-CPACG) and the eyes of normal controls.

● **METHODS:** This study included 37 patients with unilateral APAC, 37 with asymmetric CPACG without prior treatment, and 36 healthy participants. Using swept-source optical coherence tomography (SS-OCT), the macular and peripapillary choroidal thickness and three-dimensional CVI were measured and compared globally and sectorally. Pearson's correlation analysis and multivariate regression models were used to evaluate choroidal thickness or CVI with related factors.

● **RESULTS:** The mean subfoveal CVIs were 0.35±0.10, 0.33±0.09, and 0.29±0.04, and the mean subfoveal choroidal thickness were 315.62±52.92, 306.22±59.29, and 262.69±45.55 μm in the F-APAC, F-CPACG, and normal groups, respectively. All macular sectors showed significantly higher CVIs and choroidal thickness in the F-APAC and F-CPACG eyes than in the normal eyes (P<0.05), while there were no significant differences between the F-APAC and F-CPACG eyes. In the peripapillary region, the mean overall CVIs were 0.21±0.08, 0.20±0.08, and 0.19±0.05, and the mean overall choroidal thickness were 180.45±54.18, 174.82±50.67, and 176.18±37.94 μm in the F-APAC, F-CPACG, and normal groups, respectively. There were no significant differences between any of the two groups in all peripapillary sectors. Younger age, shorter axial length, and the F-APAC or F-CPACG diagnosis were significantly associated with higher subfoveal CVI and thicker subfoveal choroidal thickness (P<0.05).

● **CONCLUSION:** The fellow eyes of unilateral APAC or asymmetric CPACG have higher macular CVI and choroidal thickness than those of the normal controls. Neither CVI nor choroidal thickness can distinguish between eyes predisposed to APAC or CPACG. A thicker choroid with a higher vascular volume may play a role in the pathogenesis of primary angle-closure glaucoma.

● **KEYWORDS:** choroidal thickness; choroidal vascularity index; swept-source optical coherence tomography; acute primary angle-closure; chronic primary angle-closure glaucoma

DOI:10.18240/ijo.2024.01.06

Citation: Huang HL, Wang GH, Niu LL, Sun XH. Three-dimensional choroidal vascularity index and choroidal thickness in fellow eyes of acute and chronic primary angle-closure using swept-source optical coherence tomography. *Int J Ophthalmol* 2024;17(1):42-52

INTRODUCTION

Primary angle-closure disease (PACD) is a leading cause of irreversible blindness worldwide[1]. It is estimated that there are 25 million patients with PACD worldwide and more than 25% progress to blindness[2]. PACD, a general reference to three continuum categories, including primary angle-closure suspect (PACS), primary angle-closure (PAC), and primary angle-closure glaucoma (PACG), is characterized by

mechanical obstruction of the trabecular meshwork by either apposition of the peripheral iris to the trabecular meshwork or by a synechial closed angle[3]. Acute and chronic forms are further distinguished according to the clinical manifestations and severity of disease onset. Patients with an acute attack experience a sudden, symptomatic elevation in intraocular pressure (IOP), with the iris quickly covering the entire trabecular meshwork[4]. In the chronic form, IOP increases slowly in a painless and asymptomatic manner, with the iris gradually covering the trabecular meshwork portion by portion[5].

A shallow anterior chamber, great lens thickness, anterior lens position, short axial length, advanced age, and female sex are considered common risk factors for PACD[6]. Researchers have found that acute primary angle-closure (glaucoma) [APAC(G)] eyes have a smaller anterior chamber depth, greater lens vault, and thicker peripheral iris than chronic primary angle-closure (glaucoma) [CPAC(G)] eyes[7-8]. Recently, choroidal expansion was reported to play a role in PACD. A few studies have demonstrated greater baseline choroidal thickness in subtypes of PACDs and hypothesized that a thicker choroid which results in a greater tendency of choroidal expansion could push the lens-iris diaphragm forward, initiating or exacerbating the closure of the anterior chamber angle[9-10]. Additionally, as eyes with PACD are anatomically smaller, the expansion of the choroid may reduce the intraocular volume and therefore increase the IOP[6]. However, there has been little research comparing choroids between eyes with APAC(G) and those with CPAC(G). In addition to choroidal thickness, other choroidal parameters have rarely been explored in the population with PACD.

The recent development of optical coherence tomography (OCT) has enabled the observation of the choroid. Compared to spectral-domain OCT (SD-OCT), swept-source OCT (SS-OCT) with a longer wavelength of approximately 1050 nm further improves penetration through the retinal pigment epithelium and enables better visualization of the full-thickness choroid[11]. Choroidal thickness has been widely used to assess choroids. However, the choroid is composed of connective tissue, blood vessels, and melanocytes. Therefore, choroidal thickness measurements do not fully reflect the status of the choroidal vasculature. The choroidal vascularity index (CVI) emerges as a novel choroidal vascularity marker that accurately reflects the relationship between the luminal volume of choroidal vascular and the total choroidal volume[12-13]. Using SS-OCT, three-dimensional CVI can be generated to provide a more comprehensive evaluation of the choroidal vasculature.

In this study, we assessed the choroid in the fellow eyes of patients with unilateral APAC (F-APAC) and asymmetric CPACG (F-CPACG). The choroid is a highly vascular structure with variable parameters regulated by various factors. Previous studies have demonstrated the effects of elevated IOP[14-15], topical antiglaucoma drugs[16], and optic atrophy[17-18] on choroids. In APAC or CPACG eyes, these changes can impede the original anatomical characteristics of the choroid. In addition, media opacities such as glaucomatous flecks and corneal edema make it difficult to obtain a clear image of the choroid using OCT. PACD has been described as a bilateral condition due to high anatomical similarities, and the fellow eye could therefore perform better in evaluating the initial anatomic configuration of severely affected eyes[19-21]. Previous studies have compared the differences between F-APAC and F-CAPCG in anterior segment parameters using ultrasound biomicroscopy[22-23], but no study has compared posterior segment parameters in F-APAC and F-CAPCG eyes.

This study aimed to investigate the three-dimensional CVI and choroidal thickness in F-APAC and F-CPACG eyes using SS-OCT, comparing them with normal eyes to identify the anatomical structural differences among the population with PACD.

SUBJECTS AND METHODS

Ethical Approval This study was approved by the Human Research Ethics Committee of the Eye and ENT Hospital of Fudan University (Ethics approval number: 2021045) and adhered to the tenets of the Declaration of Helsinki. Written informed consent was obtained from all the participants.

Participants Patients diagnosed with unilateral APAC and asymmetric CPACG were recruited from the Glaucoma Clinic at Eye and ENT Hospital of Fudan University between November 2021 and November 2022. The APAC was defined according to the following criteria: 1) the presence of at least two of the following symptoms: ocular or periocular pain, nausea and/or vomiting, ipsilateral migraine, or antecedent history of intermittent blurring of vision with halos; 2) IOP spike more than 30 mm Hg; 3) the presence of at least three of the following signs: obvious conjunctival hyperemia, corneal epithelial edema, enlarged pupil, direct disappearance of light reflex, and shallow anterior chamber; 4) an occluded angle verified by gonioscopy. CPACG was defined as follows: 1) absence of symptoms of an acute attack or signs indicative of prior acute attacks; 2) more than three cumulative clock-hours peripheral anterior synechiae; 3) a chronically elevated IOP (>21 mm Hg); 4) glaucomatous optic neuropathy or visual field defect.

The fellow eyes of APAC (F-APAC) or CPACG (F-CPACG) were enrolled if 1) present or previous acute attack was absent; 2) narrow-angle (>180° of the posterior pigmented trabecular meshwork not visible by non-indentation gonioscopy), no or less than three cumulative clock-hours peripheral anterior synechiae; 3) no glaucomatous optic neuropathy or visual field

defect. To limit potential changes in the choroidal structure, no treatment, including topical antiglaucoma eye drops, laser, or intraocular surgery, was administered to the F-APAC and F-CPACG eyes. Systematic drugs, such as mannitol, were used if necessary.

Based on the International Society of Geographic and Epidemiologic Ophthalmology classification[3], the enrolled F-APAC and F-CPACG eyes were further defined as having PACS and PAC. PACS was defined as having only appositional contact between the peripheral iris and the posterior trabecular meshwork, while PAC was defined as having iridotrabecular contact, an elevated IOP or peripheral anterior synechiae with no secondary cause, and without glaucomatous optic neuropathy.

Participants with any of the following criteria were excluded: 1) secondary angle closure caused by lens subluxation, uveitis, iris neovascularization, tumor, or significant cataract with intumescent lens; 2) the use of topical antiglaucoma medicine in F-APAC and F-CPACG eyes, or prior laser or intraocular surgery; 3) diabetes or systemic hypertension; 4) high myopia or hyperopia with a spherical equivalent refractive error greater than ±6 diopters (D); 5) corneal, retinal pathology or ocular trauma; 6) inability to tolerate gonioscopy or ultrasound biomicroscopy examination, low-quality images or unstable fixation due to clinically relevant opacities of the optical media such as severe cataract. The healthy participants included in this study had mild-to-moderate cataracts but no other eye diseases. One eye from the normal control group was randomly chosen for the study.

Methods All the enrolled participants underwent comprehensive ophthalmological examinations at baseline, including best-corrected visual acuity in logMAR, slit-lamp biomicroscopy, and static and dynamic gonioscopy using a gonioscope (Volk G-1 trabeculum; Volk Optical, Inc., Mentor, OH, USA). The anterior chamber angle was graded using the modified Shaffer grading system. The IOP was measured using Goldmann applanation tonometry, and the mean value of three measurements recorded for each eye was used. Low-coherence interferometry (LenStar 900; Haag-Streit, Koeniz, Switzerland) was used to determine the axial length, central corneal thickness, lens thickness, and anterior chamber depth.

SS-OCT (VG200S; SVision Imaging, Henan, China) was performed on all patients by the same examiner (Huang HL). Two scans, one macular scan centered on the fovea (6 mm× 6 mm protocol) and one peripapillary scan centered on the optic disc (6 mm× 6 mm protocol), were acquired. In the macular region, three concentric zones were defined according to the Early Treatment Diabetic Retinopathy Study grid: fovea (diameter 1 mm), parafovea (diameter 1-3 mm), and perifovea (diameter 3-6 mm). The parafoveal and perifoveal zones were further divided into four 90° sectors each: paratemporal (paraT), peritemporal (periT), parasuperior (paraS), perisuperior (periS), paranasal (paraN), perinasal (periN), parainferior (paraI), and periinferior (periI) areas. In the peripapillary region, the choroid was measured in an annular ring with a diameter of 2-4 mm, which was automatically divided into eight sectors using the software: temporal lower (TL), temporal upper (TU), superotemporal (ST), superonasal (SN), nasal upper (NU), nasal lower (NL), inferonasal (IN), and inferotemporal (IT) areas. On SS-OCT, the choroid was defined as the volume from the basal border of the retinal pigment epithelium-Bruch membrane complex to the chorioscleral junction. The VG200S vanGogh software uses artificial intelligence algorithms to detect the contours of the large and medium-sized choroidal vessels in the B-scans and then builds the vessel morphology through three-dimensional reconstruction to achieve quantification of the large and medium-sized choroidal vessels. The three-dimensional CVI was calculated as the ratio of the choroidal vascular luminal volume to the total choroidal volume, providing an assessment of the volumetric choroidal vascular density. A color-coded map was generated to visualize the CVI for each A-scan (Figure 1).

Statistical Analysis All analyses were performed using the SPSS software package version 23.0. Data are presented as mean±standard deviation (SD) where applicable. An independent sample *t*-test was used to assess the differences in the means between the two groups. Categorical variables such as sex were assessed individually using Fisher's exact test. Pearson's correlation analysis was performed to examine the associations among age, systolic blood pressure, diastolic blood pressure, IOP at imaging, spherical equivalent, axial length, anterior chamber depth, lens thickness, and subfoveal CVI or choroidal thickness. A multiple linear regression analysis was employed to identify the factors independently associated with CVI and choroidal thickness. The model included the diagnosis, age, sex, spherical equivalent, axial length, and anterior chamber depth. For all tests, $P<0.05$ was considered to be statistically significant.

RESULTS

Patients' Demographic Data A total of 110 participants met the inclusion criteria and participated in this study. Among these, 37 participants had F-APAC (37 eyes, 33.64%), 37 had F-CPACG (37 eyes, 33.64%), and 36 participants (36 eyes, 32.73%) were enrolled as normal controls. The clinical characteristics of the study participants are summarized in Table 1. There were no significant differences in sex, mean age, systolic blood pressure, or diastolic blood pressure between any of the two groups.

Compared to the normal controls, the participants in the F-CPACG group had higher IOP at imaging ($P=0.002$)

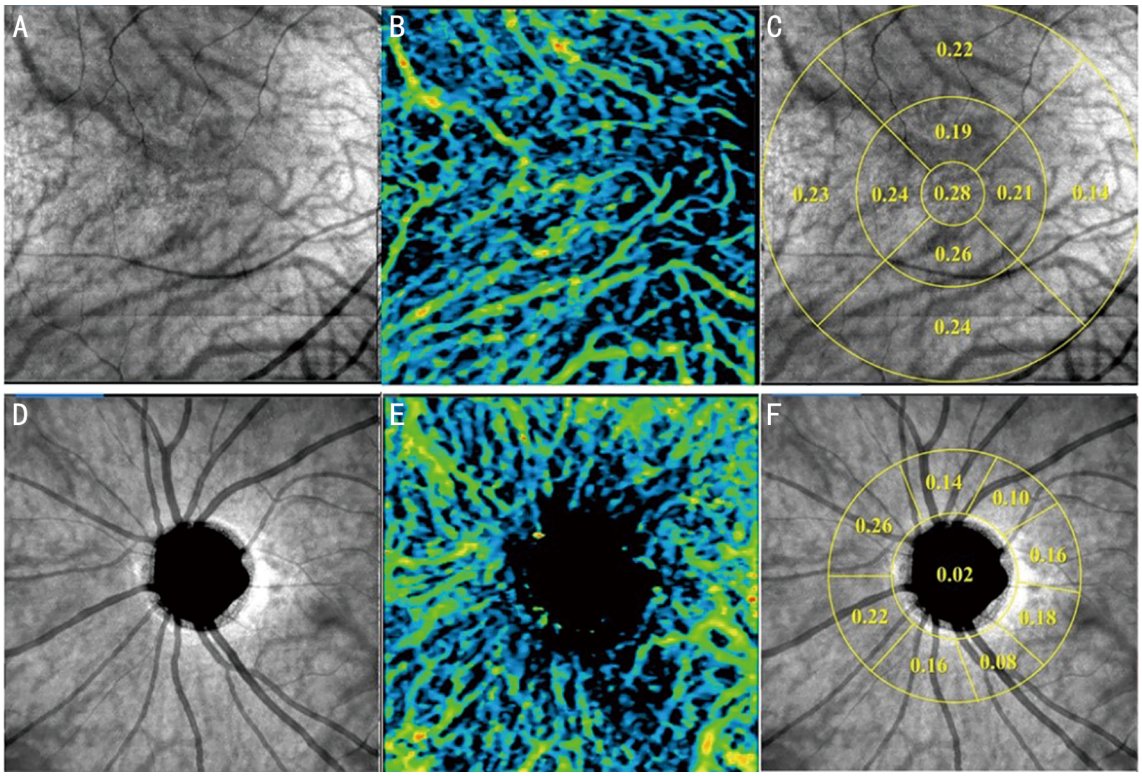

Figure 1 SS-OCT scans showing the macular and peripapillary CVI of a control eye A, D: En-face images obtained from the macular (A) and peripapillary (D) scans; B, E: Color-coded maps of the 6 mm×6 mm area were generated to show the macular (B) and peripapillary (E); C, F: The mean CVI values in the macular (C) and peripapillary (F) region. The macular region was divided into nine sectors consisting of three concentric rings with diameters of 1 mm (fovea), 1-3 mm (parafovea), and 3-6 mm (perifovea), and the peripapillary region was divided into eight sectors. SS-OCT: Swept-source optical coherence tomography; CVI: Choroidal vascularity index.

Table 1 Clinical characteristics of study participants mean±SD

Characteristics	F-APAC	F-CPACG	Normal	P^1	P^2	P^3
Patients (eyes), *n*	37 (37)	37 (37)	36 (36)	-	-	-
Age, y	60.43±8.42	61.14±8.47	60.03±5.65	0.693	0.822	0.537
Sex, male/female	13/24	14/23	13/23	0.500[a]	0.562[a]	0.536[a]
Systolic blood pressure, mm Hg	118.54±9.17	119.03±8.62	117.25±10.84	0.827	0.566	0.430
Diastolic blood pressure, mm Hg	71.65±6.39	72.81±5.50	70.75±7.17	0.435	0.549	0.171
IOP, mm Hg	14.48±4.22	17.86±4.78	14.88±3.00	0.001	0.670	0.002
Cup-to-disc ratio	0.36±0.06	0.44±0.11	0.33±0.72	<0.001	0.194	<0.001
Spherical equivalent, D	0.97±0.77	0.94±0.49	0.41±0.52	0.812	<0.001	<0.001
Axial length, mm	22.31±0.58	22.63±0.56	23.10±0.43	0.012	<0.001	<0.001
Anterior chamber depth, mm	1.93±0.19	2.12±0.23	2.49±0.38	0.005	<0.001	<0.001
Lens thickness, mm	5.03±0.32	4.92±0.25	4.74±0.31	0.113	<0.001	0.008

P^1: F-APAC *vs* F-CPACG, P^2: F-APAC *vs* normal, P^3: F-CPACG *vs* normal by using independent sample *t*-test or [a]Fisher's exact test. P<0.05 indicated statistically significant. F-APAC: Fellow eyes of acute primary angle-closure; F-CPACG: Fellow eyes of chronic primary angle-closure glaucoma; IOP: Intraocular pressure.

and bigger cup-to-disc ratio (P<0.001), while there was no significant difference between F-APAC eyes and normal eyes. Both F-APAC (P<0.001) and F-CPACG (P<0.001) groups had significantly larger spherical equivalents than the normal group, as well as thicker lens thickness. The F-APAC eyes had the shortest axial length and anterior chamber depth, followed by the F-CPACG group and the normal eyes (Table 1).

Macular and Peripapillary Measurement of the CVI and Choroidal Thickness The mean subfoveal CVIs were 0.35±0.10, 0.33±0.09, and 0.29±0.04 in the F-APAC, F-CPACG, and normal groups, respectively. All nine sectors in the macular region showed significantly higher CVI in the F-APAC and F-CAPCG eyes than in the normal eyes (P<0.05; Figure 2), and no significant differences were observed between the F-APAC and F-CPACG eyes. In all three groups, the mean CVI in the subfoveal sector was the largest and

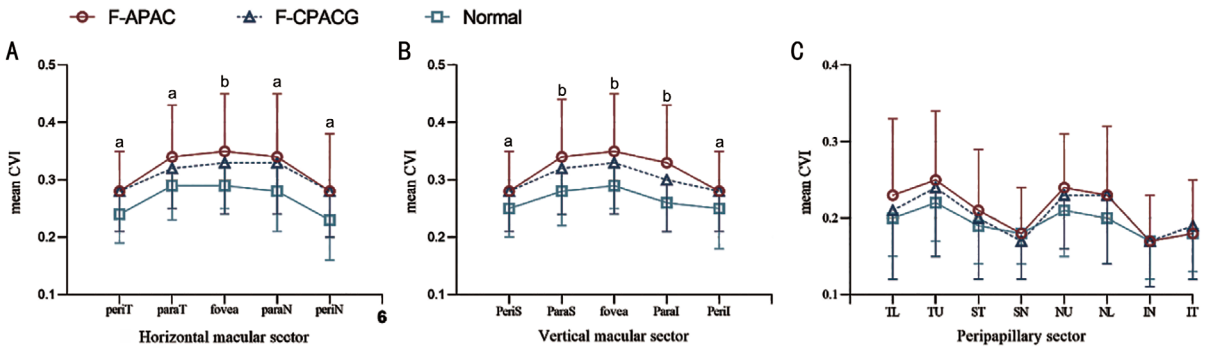

Figure 2 The mean CVI at different locations in the macular and peripapillary zone [a]*P*<0.05, [b]*P*<0.01. F-APAC: Fellow eyes of acute primary angle-closure; F-CPACG: Fellow eyes of chronic primary angle-closure glaucoma; CVI: Choroidal vascularity index; PeriT: Peritemporal; ParaT: Paratemporal; ParaN: Paranasal; PeriN: Perinasal; PeriS: Perisuperior; ParaS: Parasuperior; ParaI: Parainferior; PeriI: Periinferior; TL: Temporal lower; TU: Temporal upper; ST: Superotemporal; SN: Superonasal; NU: Nasal upper; NL: Nasal lower; IN: Inferonasal; IT: Inferotemporal.

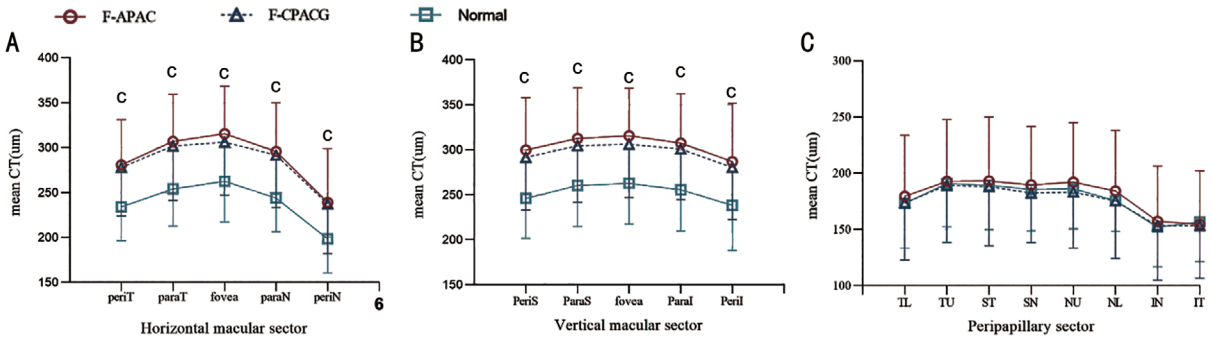

Figure 3 The mean choroidal thickness at different locations in the macular and peripapillary zone [c]*P*<0.001. F-APAC: Fellow eyes of acute primary angle-closure; F-CPACG: Fellow eyes of chronic primary angle-closure glaucoma; CT: Choroid thickness; PeriT: Peritemporal; ParaT: Paratemporal; ParaN: Paranasal; PeriN: Perinasal; PeriS: Perisuperior; ParaS: Parasuperior; ParaI: Parainferior; PeriI: Periinferior; TL: Temporal lower; TU: Temporal upper; ST: Superotemporal; SN: Superonasal; NU: Nasal upper; NL: Nasal lower; IN: Inferonasal; IT: Inferotemporal.

gradually decreased from the fovea to the distal region. In the peripapillary region, the mean overall CVIs were 0.21±0.08, 0.20±0.08, and 0.19±0.05 in the F-APAC, F-CPACG, and normal groups, respectively; however, there were no significant differences between any of the two groups in the eight peripapillary sectors. The macular and peripapillary CVI data for all sectors in the three groups are listed in Table 2.

Choroidal thickness was also measured in the macular and peripapillary regions. The mean subfoveal choroidal thickness was 315.62±52.92, 306.22±59.29, and 262.69±45.55 μm in the F-APAC, F-CPACG, and normal groups, respectively. All nine sectors in the macular region showed a significantly higher choroidal thickness in the F-APAC and F-CPACG eyes than in the normal eyes (*P*<0.05; Figure 3), and no significant difference was found between the F-APAC and F-CPACG groups. In all three groups, the mean choroidal thickness in the subfoveal sector was the highest, whereas that in the perinasal sector was the lowest. The choroidal thickness gradually decreases from the fovea to the distal region. In the peripapillary region, the mean overall choroidal thickness was 180.45±54.18, 174.82±50.67, and 176.18±37.94 μm in the F-APAC, F-CPACG, and normal groups, respectively. There were no significant differences in mean choroidal thickness between any of the two groups in the eight peripapillary sectors. Macular and peripapillary choroidal thickness data for all sectors in the three groups are listed in Table 3. In every sector, the choroidal thickness was always slightly higher in the F-APAC eyes than in the F-CPACG eyes. Figure 4 shows examples of SS-OCT-derived macular choroidal thickness and CVI obtained from control and F-APAC eyes.

Pearson Correlation Analysis The results of the Pearson correlation analysis of the subfoveal CVI and choroidal thickness are shown in Table 4. Age, spherical equivalent, axial length, and anterior chamber depth were significantly associated with subfoveal CVI and choroidal thickness in all participants (*P*<0.05). The IOP on imaging, cup-to-disc ratio, lens thickness, systolic blood pressure, and diastolic blood pressure were not correlated with CVI or choroidal thickness in the subfoveal sector.

Multiple Linear Regression Analysis Multiple linear regression analysis, including all participants, was performed to determine the factors independently associated with subfoveal CVI and choroidal thickness (Table 5). The model included diagnosis (F-APAC or F-CPACG *vs* normal), age,

Table 2 Comparison of the macular and peripapillary CVI between F-APAC eyes, F-CPACG eyes, and normal control eyes

Parameters	F-APAC	F-CPACG	Normal	P^1	P^2	P^3
Macular						
Subfoveal	0.35±0.10	0.33±0.09	0.29±0.04	0.296	0.001	0.023
ParaT	0.34±0.09	0.32±0.07	0.29±0.06	0.427	0.005	0.039
PeriT	0.28±0.07	0.28±0.07	0.24±0.05	0.929	0.019	0.024
ParaS	0.34±0.10	0.32±0.08	0.28±0.06	0.199	0.001	0.026
PeriS	0.28±0.07	0.28±0.07	0.25±0.05	0.828	0.044	0.026
ParaN	0.34±0.11	0.33±0.09	0.28±0.07	0.493	0.007	0.042
PeriN	0.28±0.10	0.28±0.08	0.23±0.07	0.814	0.017	0.031
ParaI	0.33±0.10	0.30±0.09	0.26±0.05	0.287	0.001	0.026
PeriI	0.28±0.07	0.28±0.07	0.25±0.07	0.907	0.025	0.033
Peripapillary						
TL	0.23±0.10	0.21±0.09	0.20±0.05	0.554	0.226	0.531
TU	0.25±0.09	0.24±0.09	0.22±0.05	0.496	0.063	0.233
ST	0.21±0.07	0.20±0.08	0.19±0.05	0.648	0.123	0.274
SN	0.18±0.06	0.17±0.05	0.18±0.04	0.352	0.766	0.530
NU	0.24±0.07	0.23±0.07	0.21±0.06	0.408	0.079	0.344
NL	0.23±0.09	0.23±0.09	0.20±0.06	0.953	0.122	0.108
IN	0.17±0.06	0.17±0.06	0.17±0.05	0.871	0.867	0.742
IT	0.18±0.07	0.19±0.07	0.18±0.05	0.816	0.889	0.711

P^1: F-APAC *vs* F-CPACG, P^2: F-APAC *vs* normal, P^3: F-CPACG *vs* normal. P<0.05 indicated statistically significant. F-APAC: Fellow eyes of acute primary angle-closure; F-CPACG: Fellow eyes of chronic primary angle-closure glaucoma; CVI: Choroidal vascularity index; ParaT: Paratemporal; PeriT: Peritemporal; ParaS: Parasuperior; PeriS: Perisuperior; ParaN: Paranasal; PeriN: Perinasal; ParaI: Parainferior; PeriI: Periinferior; TL: Temporal lower; TU: Temporal upper; ST: Superotemporal; SN: Superonasal; NU: Nasal upper; NL: Nasal lower; IN: Inferonasal; IT: Inferotemporal.

Table 3 Comparison of the macular and peripapillary choroidal thickness between F-APAC eyes, F-CPACG eyes, and normal control eyes

Parameters	F-APAC	F-CPACG	Normal	P^1	P^2	P^3
Macular						
Subfoveal	315.62±52.92	306.22±59.29	262.69±45.55	0.447	<0.001	0.001
ParaT	306.92±52.42	301.68±60.44	253.97±41.47	0.666	<0.001	<0.001
PeriT	280.78±50.20	277.92±54.10	234.14±37.78	0.798	<0.001	<0.001
ParaS	312.57±56.53	304.57±63.01	260.28±45.63	0.537	<0.001	0.001
PeriS	299.70±58.22	291.38±58.27	245.89±44.22	0.509	<0.001	<0.001
ParaN	295.78±54.26	291.57±58.24	243.81±37.71	0.723	<0.001	<0.001
PeriN	239.11±59.78	237.38±55.22	198.53±37.79	0.886	0.001	0.002
ParaI	307.35±55.09	300.73±56.29	255.47±45.76	0.590	<0.001	<0.001
PeriI	286.76±64.79	280.24±57.94	238.14±50.13	0.630	0.001	0.002
Peripapillary						
TL	179.65±54.06	173.76±51.02	173.25±39.88	0.604	0.576	0.965
TU	192.76±55.16	189.22±50.81	190.81±38.55	0.755	0.865	0.890
ST	193.11±56.92	188.14±52.72	189.33±39.80	0.672	0.750	0.919
SN	189.59±52.21	182.38±44.14	185.50±36.73	0.491	0.698	0.767
NU	192.16±52.90	183.22±49.80	186.25±35.51	0.413	0.590	0.782
NL	184.32±53.74	175.49±51.34	175.61±27.39	0.409	0.419	0.991
IN	157.32±48.90	153.03±48.27	151.92±35.15	0.680	0.606	0.916
IT	154.65±47.46	153.35±46.79	156.75±35.14	0.898	0.837	0.740

P^1: F-APAC *vs* F-CPACG, P^2: F-APAC *vs* normal, P^3: F-CPACG *vs* normal. P<0.05 indicated statistically significant. F-APAC: Fellow eyes of acute primary angle-closure; F-CPACG: Fellow eyes of chronic primary angle-closure glaucoma; ParaT: Paratemporal; PeriT: Peritemporal; ParaS: Parasuperior; PeriS: Perisuperior; ParaN: Paranasal; PeriN: Perinasal; ParaI: Parainferior; PeriI: Periinferior; TL: Temporal lower; TU: Temporal upper; ST: Superotemporal; SN: Superonasal; NU: Nasal upper; NL: Nasal lower; IN: Inferonasal; IT: Inferotemporal.

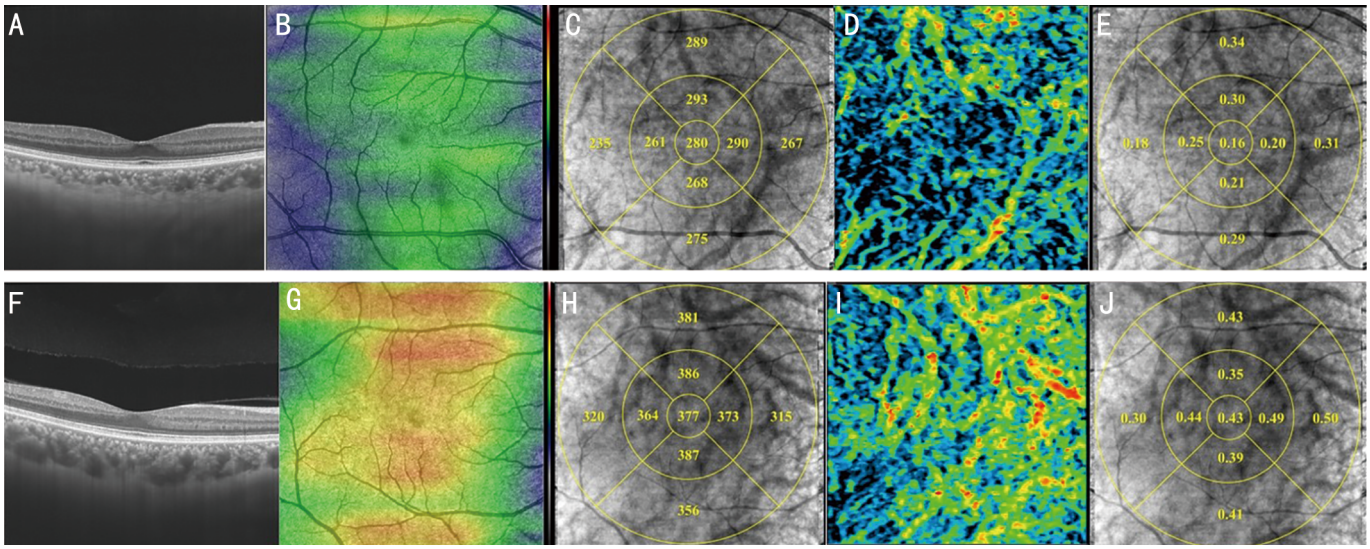

Figure 4 SS-OCT derived choroidal thickness and CVI in the macular region for a control and an F-APAC eye The F-APAC eye had a higher macular choroidal thickness and CVI than the control eye. A, F: The B scan images of macular choroidal thickness in the control (A) and the F-APAC (F) eye; B, G: Color-coded maps of the macular choroidal thickness obtained from the control (B) and the F-APAC (G) eye; C, H: The mean choroidal thickness values in the nine sectors of the macular region in the control (C) and the F-APAC (H) eye; D, I: Color-coded maps of the macular CVI obtained from the control (D) and the F-APAC (I) eye; E, J: The mean CVI values in the nine sectors of the macular region in the control (E) and the F-APAC (J) eyes. SS-OCT: Swept-source optical coherence tomography; CVI: Choroidal vascularity index; F-APAC: Fellow eyes of acute primary angle-closure; F-CPACG: Fellow eyes of chronic primary angle-closure glaucoma.

Table 4 Pearson correlation analysis of the subfoveal CVI and subfoveal choroidal thickness in all eyes

Factors	Subfoveal CVI		Subfoveal choroidal thickness, μm	
	r	*P*	*r*	*P*
Age, y	-0.319	0.001	-0.283	0.003
Systolic blood pressure, mm Hg	0.105	0.274	0.066	0.495
Diastolic blood pressure, mm Hg	0.138	0.150	0.164	0.086
IOP, mm Hg	0.055	0.566	0.169	0.078
Cup-to-disc ratio	-0.051	0.596	-0.032	0.738
Spherical equivalent, D	0.296	0.002	0.343	<0.001
Axial length, mm	-0.358	<0.001	-0.471	<0.001
Anterior chamber depth, mm	-0.251	0.008	-0.376	<0.001
Lens thickness, mm	0.062	0.521	-0.001	0.994

P<0.05 indicated statistically significant. CVI: Choroidal vascularity index; IOP: Intraocular pressure.

Table 5 Multiple linear regression analysis of the subfoveal CVI and subfoveal choroidal thickness in all eyes

Factors	Subfoveal CVI		Subfoveal choroidal thickness, μm	
	Beta	*P*	Beta	*P*
Age, y	-0.003	0.001	-1.946	0.002
Axial length, mm	-0.030	0.02	-29.535	0.001
Diagnosis	0.037	0.036	31.154	0.006

P<0.05 indicated statistically significant. CVI: Choroidal vascularity index.

spherical equivalent, axial length, and anterior chamber depth. The results of the regression analysis showed that age (*P*=0.001), axial length (*P*=0.02), and diagnosis (*P*=0.036) were most commonly associated with subfoveal CVI. Age (*P*=0.002), axial length (*P*=0.001), and diagnosis (*P*=0.006) were significantly associated with subfoveal choroidal thickness. After adjusting for age, axial length, or diagnosis, the spherical equivalent and anterior chamber depth showed no significant correlation with the subfoveal CVI or choroidal thickness.

DISCUSSION

This study compared the three-dimensional CVI and choroidal thickness between fellow eyes of unilateral APAC and asymmetric CPACG and the eyes of normal controls. In the present SS-OCT study, F-APAC and F-CPACG eyes, defined as PACS or PAC eyes, had higher macular CVI and choroidal thickness values than the control eyes. To the best of our knowledge, this is the first study to evaluate the three-dimensional choroidal vasculature among the population with PACD and also the first to compare choroidal parameters

among the fellow eyes of APAC(G) and CPAC(G) before any treatment.

The anatomical characteristics of choroid would have changed remarkably after IOP elevation, the use of anti-glaucoma eye drops, and even optic atrophy[14-16], making it unable to represent the original anatomical structures before the disease develops in eyes with APAC and CPACG eyes. In addition, it's difficult to obtain clear choroidal images due to media opacity, such as glaucomatous flecks and corneal edema caused by elevated IOP, in the severely affected eyes with APAC and CPACG eyes. PACD is considered to be a bilateral condition with asymmetric severity between eyes. Untreated eyes with PACS have a 22% 5-year incidence of PAC, progression to PACG has been noted in 28.5% of eyes with PAC[24-25]. Owing to high anatomical similarities, the fellow eye could better reflect the original anatomical structure of the severely affected eyes[19-21]. Based on the above deduction, we chose the fellow untreated and less-affected eyes of APAC and CPACG, and our results indicate that a thicker choroid with a higher vascular volume is an inherent anatomical structure of the population with PACD and might play a role in disease pathogenesis.

In previous studies, histology was used to analyze the choroid, which has a limited scope of application because of its invasiveness and postmortem changes in choroidal blood flow[26-28]. OCT and OCT angiography also have limited applications because of their artifacts, which are easily affected by the refractive media and the limited detection area of the macula and peripapillary choroid[29-31]. SD-OCT and SS-OCT are emerging technologies that can generate high-resolution full-thickness choroid images based on longer-wavelength light use and higher penetration at the retinal pigment epithelium and are more suitable for evaluating the choroid[32-33]. Compared to SD-OCT, SS-OCT at a 1050-nm wavelength further improves penetration and resolution, enables better visualization and more accurate evaluation of the full-thickness choroid[11,34], and is more suitable for generating three-dimensional CVI.

In previous studies, choroidal thickness was often measured by selecting several points, such as the fovea and a few points from different quadrants around the macula or optic disc[35-38]. However, the highly vascularized choroid tissue is partially irregular; therefore, such methods may not display all dimensions of the choroid. In this study, we used the average choroidal thickness of a specific sector to calculate the mean choroidal thickness of each A-scan within the target area. Compared to the traditional measurement method, this method further reduces data loss and selection errors. In our study, choroidal thickness in all nine macular sectors showed significantly higher values in the F-APAC and F-CPACG eyes than in normal eyes, but there were no significant differences between any of the two groups in the peripapillary sectors. In all three groups, the mean choroidal thickness in the subfoveal sector was the highest, whereas that in the perinasal sector was the lowest. The thickness of the choroid gradually decreases from the fovea to the distal region. The multivariate linear regression analysis showed that age, axial length, and F-APAC or F-CAPCG diagnosis were significantly associated with subfoveal choroidal thickness. These results are comparable with previous studies[35-38].

In addition to choroidal thickness, we used the CVI parameter to assess choroids in patients with PACD. This is because CVI is an accurate and stable parameter for evaluating choroidal vasculature and is influenced by fewer physiological factors than choroidal thickness; CVI is determined by both anatomical structure and blood flow[11-12]. We replaced the traditional method with a three-dimensional CVI[39-40]. Previous studies have evaluated only a limited region of the choroidal vasculature using two-dimensional images. To comprehensively evaluate the choroidal vasculature, the three-dimensional CVI was used to provide more accurate measurements. In the current study, all nine sectors in the macular region showed significantly higher CVIs in the F-APAC and F-CPACG eyes than in the normal eyes. Multiple regression analysis showed that age, axial length, and F-APAC or F-CAPCG diagnosis were significantly associated with subfoveal CVI. The potential role of higher choroidal vasculature volume as a risk factor for PACD must be further investigated. Further studies are required to reveal the spatial correlation between CVI and clinical features such as visual field damage or retinal nerve fiber layer thinning.

Although some anterior segment parameters, such as iris curvature, iris-ciliary process distance, and anterior chamber depth[22-23], can distinguish eyes predisposed to APAC or CPACG, in our study, no significant differences were found in choroidal thickness and CVI between F-APAC eyes and F-CPACG eyes. This suggests that the choroidal parameters could not predict the occurrence of APAC. However, we noticed that the mean choroidal thickness and CVI values of every sector, without exception, were slightly higher in F-APAC eyes than in F-CPACG eyes. This indicates that a thicker choroid with higher vasculature may play a role in acute attack onset.

In this study, we found that not only was choroidal thickness an independent risk factor, but that increased CVI could also play a role in the pathogenesis of PACD. The choroid is a highly vascularized layer located between the retina and sclera, and choroidal overperfusion may cause increased choroidal thickness. Choroid expansion is expected to push the lens-iris diaphragm forward because of the relatively rigid sclera and cornea, initiating or aggravating the angle-closure process[9]. Simultaneously, choroidal expansion can reduce

intraocular volume, thereby increasing IOP[41]. Meanwhile, the population with PACD has the anatomic characteristics of a smaller eyeball, a shorter axial length, and a shallow anterior chamber[6]. Eyes with these anatomic abnormalities tend to have thicker choroids[42]; therefore, when the choroids further expand in this population, it will be easier to cause an angle closure onset and IOP increase compared with healthy people. Furthermore, we speculated that because the choroid itself is the pathway for the outflow of aqueous humor, the balance between IOP and choroidal perfusion pressure directly affects the outflow of aqueous humor[43-44]. Therefore, resistance to the outflow of aqueous humor due to increased CVI could cause the IOP to increase and promote the process of angle closure, thereby inducing the onset of PACD. Therefore, based on the underlying mechanism, we determined that there is a theoretical basis for exploring choroidal vascular status in PACD by assessing CVI and choroidal thickness.

The limitations of this study are as follows: 1) The small test population may have led to selection errors. This study only included patients with PACS and PAC and did not include patients who had entered the clinical stage of glaucoma. Therefore, we could not study the relationship between the choroid and the different clinical stages of angle-closure glaucoma. 2) To date, there is not an unified detection method to distinguish the choriocapillaris, Sattler layer, and Haller layer of the choroid[45-46]; therefore, it is still unclear which layer of the choroid is involved in the process of PACD. In the future, more advanced detection methods should be developed to illustrate this issue better. 3) The choroidal thickness and blood flow change dynamically with other factors, such as the time of day, body position, mood, and body temperature[47-48], which added contingency to our results and made the abnormal changes in the choroid outside the observation time easy to ignore. To address this issue, further 24-hour choroid monitoring to observe the choroid at different times during the day may be required. In addition, although no local drugs were administered directly to the fellow eyes, the drug effects on the fellow eyes and systemic drug effects were difficult to evaluate in our study. 4) This study demonstrated that changes in choroidal thickness and CVI are characteristics of the contralateral eyes of APAC and CPACG but did not clarify the causal relationship, that is, whether choroid changes lead to angle closure. Although rigorous theoretical speculation has been made, exact causality must be clarified through longitudinal cohort studies.

In summary, the fellow eyes of patients with unilateral APAC and asymmetric CPACG had greater macular choroidal thickness and increased macular CVI than the normal control eyes. However, neither CVI nor choroidal thickness can distinguish between eyes predisposed to APAC and those predisposed to CPACG. These changes were independent of confounding factors such as age and axial length, indicating that a thicker choroid with higher vasculature volume may be an inherent anatomical characteristic of eyes with PACD and may play a role in the pathogenesis.

ACKNOWLEDGEMENTS

Authors' contributions: Concept and design: Huang HL, Sun XH; data collection: Huang HL, Wang GH; analysis and interpretation: Wang GH, Niu LL; writing the article: Huang HL, Wang GH; critical revision: Sun XH; final approval: all authors.

Foundations: Supported by the National Natural Science Foundation of China (No.82101087); Shanghai Clinical Research Key Project (No.SHDC2020CR6029).

Conflicts of Interest: Huang HL, None; **Wang GH,** None; **Niu LL,** None; **Sun XH,** None.

REFERENCES

1 Reis TF, Paula JS, Furtado JM. Primary glaucomas in adults: epidemiology and public health-a review. *Clin Exp Ophthalmol* 2022;50(2):128-142.

2 Bourne RRA, Flaxman SR, Braithwaite T, Cicinelli MV, Das A, Jonas JB, *et al*. Magnitude, temporal trends, and projections of the global prevalence of blindness and distance and near vision impairment: a systematic review and meta-analysis. *Lancet Glob Health* 2017;5(9):e888-e897.

3 Foster PJ, Buhrmann R, Quigley HA, Johnson GJ. The definition and classification of glaucoma in prevalence surveys. *Br J Ophthalmol* 2002;86(2):238-242.

4 Chan PP, Pang JC, Tham CC. Acute primary angle closure-treatment strategies, evidences and economical considerations. *Eye (Lond)* 2019;33(1):110-119.

5 Sun X, Ji X, Zheng Y, Guo B. Primary chronic angle-closure glaucoma in Chinese—a clinical exploration of its pathogenesis and natural course. *Yan Ke Xue Bao* 1994;10(3):176-185.

6 Stein JD, Khawaja AP, Weizer JS. Glaucoma in adults-screening, diagnosis, and management: a review. *JAMA* 2021;325(2):164-174.

7 Guzman CP, Gong T, Nongpiur ME, *et al*. Anterior segment optical coherence tomography parameters in subtypes of primary angle closure. *Invest Ophthalmol Vis Sci* 2013;54(8):5281-5286.

8 Moghimi S, Vahedian Z, Fakhraie G, Ghaffari R, Eslami Y, Jabarvand M, Zarei R, Mohammadi M, Lin S. Ocular biometry in the subtypes of angle closure: an anterior segment optical coherence tomography study. *Am J Ophthalmol* 2013;155(4):664-673.e1.

9 Nguyen DT, Giocanti-Aurégan A, Benhatchi N, *et al*. Increased choroidal thickness in primary angle closure measured by swept-source optical coherence tomography in Caucasian population. *Int Ophthalmol* 2020;40(1):195-203.

10 Sun X, Dai Y, Chen Y, Yu DY, Cringle SJ, Chen J, Kong X, Wang X, Jiang C. Primary angle closure glaucoma: what we know and what we don't know. *Prog Retin Eye Res* 2017;57:26-45.

11 Laíns I, Wang JC, Cui Y, Katz R, Vingopoulos F, Staurenghi G, Vavvas DG, Miller JW, Miller JB. Retinal applications of swept source optical coherence tomography (OCT) and optical coherence tomography angiography (OCTA). *Prog Retin Eye Res* 2021;84:100951.

12 Iovino C, Pellegrini M, Bernabei F, *et al*. Choroidal vascularity index: an in-depth analysis of this novel optical coherence tomography parameter. *J Clin Med* 2020;9(2):595.

13 Betzler BK, Ding J, Wei X, *et al*. Choroidal vascularity index: a step towards software as a medical device. *Br J Ophthalmol* 2022;106(2):149-155.

14 Silva D, Lopes AS, Henriques S, Lisboa M, Pinto S, Trancoso Vaz F, Prieto I. Changes in choroidal thickness following trabeculectomy and its correlation with the decline in intraocular pressure. *Int Ophthalmol* 2019;39(5):1097-1104.

15 Singh N, Pegu J, Garg P, Kumar B, Dubey S, Gandhi M. Correlation between choroidal thickness and intraocular pressure control in primary angle-closure glaucoma. *Indian J Ophthalmol* 2022; 70(1):147-152.

16 Yeung SC, Park JY, Park D, You Y, Yan P. The effect of systemic and topical ophthalmic medications on choroidal thickness: a review. *Br J Clin Pharmacol* 2022;88(6):2673-2685.

17 Park KA, Choi DD, Oh SY. Macular choroidal thickness and peripapillary retinal nerve fiber layer thickness in normal adults and patients with optic atrophy due to acute idiopathic demyelinating optic neuritis. *PLoS One* 2018;13(6):e0198340.

18 Mello LGM, Suzuki ACF, de Mello GR, Preti RC, Zacharias LC, Monteiro MLR. Choroidal thickness in eyes with band atrophy of the optic nerve from chiasmal compression. *J Ophthalmol* 2022;2022:5625803.

19 Li F, Huo Y, Ma L, Yan X, Zhang H, Geng Y, Zhang Q, Tang G. Clinical observation of macular choroidal thickness in primary chronic angle-closure glaucoma. *Int Ophthalmol* 2021;41(12):4217-4223.

20 Huang J, Wang Z, Wu Z, Li Z, Lai K, Ge J. Comparison of ocular biometry between eyes with chronic primary angle-closure glaucoma and their fellow eyes with primary angle-closure or primary angle-closure suspect. *J Glaucoma* 2015;24(4):323-327.

21 Friedman DS, Gazzard G, Foster P, Devereux J, Broman A, Quigley H, Tielsch J, Seah S. Ultrasonographic biomicroscopy, Scheimpflug photography, and novel provocative tests in contralateral eyes of Chinese patients initially seen with acute angle closure. *Arch Ophthalmol* 2003;121(5):633-642.

22 Li M, Chen Y, Chen X, Zhu W, Chen X, Wang X, Fang Y, Kong X, Dai Y, Chen J, Sun X. Differences between fellow eyes of acute and chronic primary angle closure (glaucoma): an ultrasound biomicroscopy quantitative study. *PLoS One* 2018;13(2):e0193006.

23 You S, Liang Z, Yang K, Zhang Y, Oatts J, Han Y, Wu H. Novel discoveries of anterior segment parameters in fellow eyes of acute primary angle closure and chronic primary angle closure glaucoma. *Invest Ophthalmol Vis Sci* 2021;62(14):6.

24 Thomas R, George R, Parikh R, Muliyil J, Jacob A. Five year risk of progression of primary angle closure suspects to primary angle closure: a population based study. *Br J Ophthalmol* 2003; 87(4):450-454.

25 Thomas R, Parikh R, Muliyil J, Kumar RS. Five-year risk of progression of primary angle closure to primary angle closure glaucoma: a population-based study. *Acta Ophthalmol Scand* 2003;81(5):480-485.

26 Kubota T, Jonas JB, Naumann GO. Decreased choroidal thickness in eyes with secondary angle closure glaucoma. An aetiological factor for deep retinal changes in glaucoma? *Br J Ophthalmol* 1993; 77(7):430-432.

27 O'Brart DP, de Souza Lima M, Bartsch DU, Freeman W, Weinreb RN. Indocyanine green angiography of the peripapillary region in glaucomatous eyes by confocal scanning laser ophthalmoscopy. *Am J Ophthalmol* 1997;123(5):657-666.

28 Kubota T, Schlötzer-Schrehardt UM, Naumann GO, Kohno T, Inomata H. The ultrastructure of parapapillary chorioretinal atrophy in eyes with secondary angle closure glaucoma. *Graefes Arch Clin Exp Ophthalmol* 1996;234(6):351-358.

29 Lee EJ, Lee KM, Lee SH, Kim TW. Parapapillary choroidal microvasculature dropout in glaucoma: a comparison between optical coherence tomography angiography and indocyanine green angiography. *Ophthalmology* 2017;124(8):1209-1217.

30 Lee EJ, Kim S, Hwang S, Han JC, Kee C. Microvascular compromise develops following nerve fiber layer damage in normal-tension glaucoma without choroidal vasculature involvement. *J Glaucoma* 2017;26(3):216-222.

31 Suh MH, Zangwill LM, Manalastas PI, Belghith A, Yarmohammadi A, Medeiros FA, Diniz-Filho A, Saunders LJ, Weinreb RN. Deep retinal layer microvasculature dropout detected by the optical coherence tomography angiography in glaucoma. *Ophthalmology* 2016;123(12):2509-2518.

32 Damian I, Roman G, Nicoară SD. Analysis of the choroid and its relationship with the outer retina in patients with diabetes mellitus using binarization techniques based on spectral-domain optical coherence tomography. *J Clin Med* 2021;10(2):210.

33 Xie R, Qiu B, Chhablani J, Zhang X. Evaluation of choroidal thickness using optical coherent tomography: a review. *Front Med* 2021;8:783519.

34 Pinilla I, Sanchez-Cano A, Insa G, Bartolomé I, Perdices L, Orduna-Hospital E. Choroidal differences between spectral and swept-source domain technologies. *Curr Eye Res* 2021;46(2):239-247.

35 Zhou M, Wang W, Ding X, Huang W, Chen S, Laties AM, Zhang X. Choroidal thickness in fellow eyes of patients with acute primary angle-closure measured by enhanced depth imaging spectral-domain optical coherence tomography. *Invest Ophthalmol Vis Sci* 2013;54(3):1971-1978.

36 Wang YX, Xu L, Shao L, Zhang YQ, Yang H, Wang JD, Jonas JB, Wei WB. Subfoveal choroidal thickness and glaucoma. the Beijing eye study 2011. *PLoS One* 2014;9(9):e107321.

37 Zhou M, Wang W, Huang W, Gao X, Li Z, Li X, Zhang X. Is increased choroidal thickness association with primary angle closure? *Acta Ophthalmol* 2014;92(7):e514-e520.

38 Song W, Huang P, Dong X, Li X, Zhang C. Choroidal thickness decreased in acute primary angle closure attacks with elevated intraocular pressure. *Curr Eye Res* 2016;41(4):526-531.

39 Yang J, Wang E, Yuan M, Chen Y. Three-dimensional choroidal vascularity index in acute central serous chorioretinopathy using swept-source optical coherence tomography. *Graefes Arch Clin Exp Ophthalmol* 2020;258(2):241-247.

40 Xu A, Sun G, Duan C, Chen Z, Chen C. Quantitative assessment of three-dimensional choroidal vascularity and choriocapillaris flow signal voids in myopic patients using SS-OCTA. *Diagnostics* 2021;11(11):1948.

41 Quigley HA. What's the choroid got to do with angle closure? *Arch Ophthalmol* 2009;127(5):693-694.

42 Goharian I, Sehi M. Is there any role for the choroid in glaucoma? *J Glaucoma* 2016;25(5):452-458.

43 Quigley HA. Angle-closure glaucoma-simpler answers to complex mechanisms: LXVI Edward Jackson memorial lecture. *Am J Ophthalmol* 2009;148(5):657-669.e1.

44 Zhang X, Cole E, Pillar A, Lane M, Waheed N, Adhi M, Magder L, Quigley H, Saeedi O. The effect of change in intraocular pressure on choroidal structure in glaucomatous eyes. *Invest Ophthalmol Vis Sci* 2017;58(7):3278-3285.

45 Uppugunduri SR, Rasheed MA, Richhariya A, Jana S, Chhablani J, Vupparaboina KK. Automated quantification of Haller's layer in choroid using swept-source optical coherence tomography. *PLoS One* 2018;13(3):e0193324.

46 Ma DJ, Park UC, Kim ET, Yu HG. Choroidal vascularity changes in idiopathic central serous chorioretinopathy after half-fluence photodynamic therapy. *PLoS One* 2018;13(8):e0202930.

47 Li F, Li H, Yang J, Liu J, Aung T, Zhang X. Upside-down position leads to choroidal expansion and anterior chamber shallowing: OCT study. *Br J Ophthalmol* 2020;104(6):790-794.

48 Burfield HJ, Carkeet A, Ostrin LA. Ocular and systemic diurnal rhythms in emmetropic and myopic adults. *Invest Ophthalmol Vis Sci* 2019;60(6):2237-2247.